THE STUDY OF THE INFLUENCE OF BOUNDARY CONDITIONS AND HETEROGENEITY IN THE PERFORMANCE OF THE NUMERICAL UPSCALING METHOD FOR ABSOLUTE PERMEABILITY

Lindaura Maria Steffens

Rogrio Tadeu Santana Junior

lindaura.steffens@udesc.br

rogerio_rts@yahoo.com

Universidade do Estado de Santa Catarina-UDESC

CESFI, Av. Central,413, 88330-668, Balnerio Cambori, Santa Catarina, Brasil

Carolina Mendes Isidoro

isidoro.carolina@gmail.com

Universidade do Estado de Santa Catarina-UDESC

CESFI, Av. Central,413, 88330-668, Balnerio Cambori, Santa Catarina, Brasil

Abstract. *In a previous work a numerical upscaling technique for absolute permeability was developed. This method is a non-local technique that uses a cell layer around the upscaling zone to reduce boundary conditions influence. Upscaling zone is the set of cells of interest for upscaling, and the cell layers (or rings) are the adjacent cells in the fine grid. The following is an extension of the method and it studies the use of more than one ring around the upscaling zone and the effect of high heterogeneity areas in upscaling. Intuition says that a greater number of rings should improve the results, since it leads to reducing boundary conditions effect. However, the use of more layers implies in a higher complexity in the upscaling algorithm. In current study, the use of 1 and 2 rings to upscale a permeability grid was considered. Computational time and percentual error were compared for performance analysis. In addition, the method was compared to the harmonic and arithmetic average techniques. Flow simulations were performed using finite-difference method and incompressible single-phase flow based. The*

method was applied to SPE's dataset 1 and some permeability fields generated by numerical probability distribution.

Keywords: *Upscaling techniques, Absolute Permeability, Single-Phase Flow, Reservoir Simulation, Finite-Difference Method.*

1 INTRODUCTION

The main objective of reservoir flow simulations, based on conventional and unconventional techniques, is to obtain an understanding of the flow processes involved in hydrocarbon recovery to enable prediction of production volumes. These aims require numerical modelling of the mathematics and physics of the flow processes including mass balance and Darcy's law. Through advanced instruments, methods and measurements it is possible to obtain a good knowledge about hydrocarbons deposits and to make accurate three-dimensional geological models.

A geological model is required where the reservoir is described as a mesh of grid cells. The model requires input parameters such as a permeability and porosity distribution, relative permeability functions, etc. The data are obtained on a different scale, generally lower, than that used to discretize the numerical reservoir model. So many flow simulators cannot deal directly and effectively with the size of the mesh used in geological models. In fact, software for flow simulations is still limited. Therefore, an important issue in the numerical simulation of flow in reservoirs is the scale problem.

Nowadays, these models can be consist of 10 million active cells while the simulations can be performed within a reasonable time with models of the order of hundreds of cells (Christie, 1996). Unfortunately, it is impossible to run fluid flow simulations in a reasonable computational time in complicated geological models. Hence, accurate representation of the geology requires some form of averaging of parameters.

Thus, the upscaling concept arises, which is a process of obtaining a coarse mesh (low resolution - discretization scale), which is better suited to the simulation based on a fine mesh (high resolution - measurement scale). This implies a model for achieving results through simulations preserving the representative behavior, even omitting much of the fine detail of the geological model. Therefore, upscaling techniques on rock properties are used for the reduction of the geological scale, allowing production/injection flow simulations.

The upscaling process determines the effective property value of a heterogeneous model represented by a correspondent homogeneous model (Odsaeter, 2013). In this way, is possible to run fluid flow simulations with reasonable time consumption. Upscaling a fine geological model is always a fundamental and critical step in reservoir simulation processes. In other words, it is essentially an averaging procedure where those of the coarse one, as illustrated in Fig. 1, approximate the static and dynamic characteristics of the fine scale model.

The upscaling techniques range from simple averaging of heterogeneous values within the block to sophisticated inversions. The simple and combined averages methods are easy to implement and are still technical standard estimates in the oil industry, even though for many the simple average distributions are, not good estimates. For example, the geometric average of a finite fraction distribution with zero permeability is zero, even though the system may have a total permeability nonzero. To overcome this difficulty, several attempts have been made. Harmonic
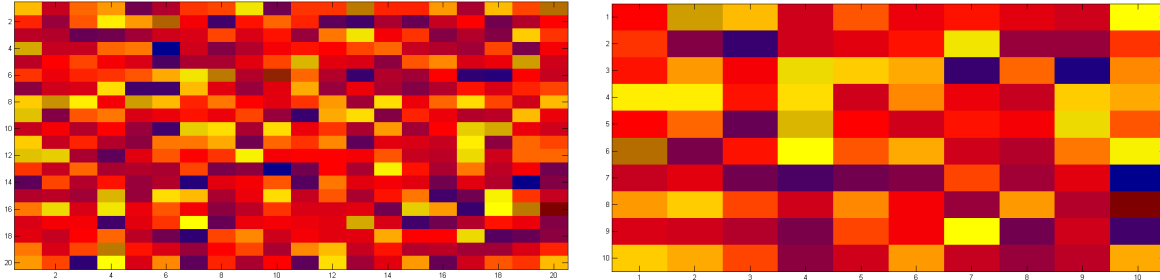
Figure 1: Example of upscaling field. The fine model (on the left) and the scaled up (on the right) obtained by applying harmonic average technique

and arithmetic average techniques are used in different cases. In fact, their application depends on the main permeability change direction. Whereas, power average includes a parameter (p) which depends on the permeability distribution. Besides, for addictive properties, it is easy to achieve a good approximation of the original fine grid. Volumetric (or additive) properties, such as porosity and saturation, do not need particular scaling technique.

Therefore, upscaling techniques are nowadays so important and cannot be avoided. However, replacing a more detailed model with an approximated one implies the loss of lots of information. The direct consequence is a lower quality prediction of flow rates and pressure distributions. Their upscale representation is given by simple averaging methods. However, when dealing with non-additive properties, such as the absolute permeability, it is not always possible to approximate effective values by simply using weighted arithmetic average techniques. In fact, in this case, the problem is complicated, it is necessary to take into account different aspects.

A great number of works in thesis and papers have been published on this subject in the last years (White and Horne (1987), Wen et al. (2003), Odsaeter (2013)). Wen and Gmez-Hernndez (1996) and Renard and Marsily (2000), present a detailed review of the main methods and procedures of the upscaling, describing its advantages and limitations. Firstly, in this work, we describe a numerical upscaling technique for absolute permeability proposed in a previous work by Failla (2015), based on single-phase flow and the finite-difference method. Posteriorly the method was applied to different problems in order to assess the influence of boundary conditions and how a larger number of cell layers would reduce this influence and improve the results.

2   PROBLEM STATEMENT

2.1   Darcy's Law

The equation that describes flow in porous medium is Darcy's Law. For this equation, some assumptions have to be made: laminar and single-phase flow, Newtonian and homogeneous fluids, no chemical and kinetic interactions between the fluid and the rock. It can be expressed mathematically as:

$$q = -\frac{k}{\mu}\frac{\partial p}{\partial s}A,\tag{1}$$

where q is the flow rate μ is the fluid viscosity, $\frac{\partial p}{\partial s}$ is the gradient of pressure, A is the cross-sectional area, and k is the absolute rock permeability.

The $Darcy velocity$ u is caculated by $u = q/A$. Rewriting:

$$u = -\frac{k}{\mu}\frac{\partial p}{\partial s}. \tag{2}$$

This equation may be written in a 3D flow system, including de gravitational term:

$$\mathbf{u} = -\frac{\mathbf{k}}{\mu}(\nabla p - \rho g \nabla h), \tag{3}$$

where $\mathbf{u} = (u_x, u_y, u_z)$ is the superficial *Darcy Velocity*, ρ is the *density of fluid* per unit volume, g is the *gravity acceleration*, h is the depth, ∇ is the *gradient* operator, and $\mathbf{k}$ is the *absolute permeability tensor*.

The permeability tensor is mathematically represented by:

$$\begin{bmatrix} k_{xx} & k_{xy} & k_{xz} \\ k_{yx} & k_{yy} & k_{yz} \\ k_{zx} & k_{zy} & k_{zz} \end{bmatrix}. \tag{4}$$

The absolute permeability is an rock property and it does not depend on pressure, temperature and fluid properties. Assuming that the coordinate system and the principal axes of the permeability tensor are aligned, results in a diagonalized permeability tensor:

$$\begin{bmatrix} k_{xx} & 0 & 0 \\ 0 & k_{yy} & 0 \\ 0 & 0 & k_{zz} \end{bmatrix}. \tag{5}$$

The absolute permeability tensor is defined for each grid-block. Thus, if the cells are isotropic, becomes $k_{xx} = k_{yy} = k_{zz}$. This is a further simplification of the analysis, valid only for the fine model, because it is commonly discretized to have homogeneous cells.

2.2 Diffusivity Equation

The mass conservation equation for porous medium is:

$$\frac{\partial(\rho\phi)}{\partial t} = -\nabla.(\rho\mathbf{u}) + \tilde{q}, \tag{6}$$

where ϕ is the porosity, $\nabla.$ is the *divergence* and $\mathbf{u} = (u_x, u_y, u_z)$ is the superficial Darcy velocity, and $\tilde{q}$ the external sources and sinks. Substituting Eq. (3) into Eq. (6) yields

$$\frac{\partial(\rho\phi)}{\partial t} = \nabla.\left(\rho\frac{\mathbf{k}}{\mu}(\nabla p - \rho g \nabla h)\right) + \tilde{q}, \tag{7}$$

this equation is called *Diffusivity Equation*. The term on right-hand side of Eq. (7) may be rewritten:

$$\frac{\partial(\rho\phi)}{\partial t} = \rho\frac{\partial\phi}{\partial t} + \phi\frac{\partial\rho}{\partial t}. \tag{8}$$

The *fluid compressibility* c_f is defined:

$$c_f = -\frac{1}{V_f}\frac{\partial V_f}{\partial p}\bigg|_T = \frac{1}{\rho}\frac{\partial\rho}{\partial p}\bigg|_T, \tag{9}$$

and the *rock compressibility* c_r is defined as:

$$c_r = \frac{1}{\phi}\frac{\partial\phi}{\partial p}. \tag{10}$$

After some manipulation, we obtain:

$$\frac{\partial\rho}{\partial t} = \rho c_f \frac{\partial p}{\partial t}, \tag{11}$$

$$\frac{\partial\phi}{\partial t} = \phi c_r \frac{\partial p}{\partial t}. \tag{12}$$

Substituting Eq. (12) and Eq. (11) into Eq. (7) yields

$$\rho\phi(c_r + c_f)\frac{\partial p}{\partial t} = \nabla.\left(\rho\frac{\mathbf{k}}{\mu}(\nabla p - \rho g\nabla h)\right) + \tilde{q}. \tag{13}$$

Defining the *total compressibility*:

$$c_t = c_r + c_f. \tag{14}$$

Substituing Eq. (14) into Eq. (7), we obtain:

$$\rho\phi c_t \frac{\partial p}{\partial t} = \nabla.\left(\rho\frac{\mathbf{k}}{\mu}(\nabla p - \rho g\nabla h)\right) + \tilde{q}. \tag{15}$$

Finally, expanding the equation in rectangular coordinates:

$$\rho\phi c_t\frac{\partial p}{\partial t} = \frac{\partial}{\partial x}\left(\frac{\rho k_x}{\mu}\left(\frac{\partial p}{\partial x} - \gamma\frac{\partial h}{\partial x}\right)\right) + \frac{\partial}{\partial y}\left(\frac{\rho k_y}{\mu}\left(\frac{\partial p}{\partial y} - \gamma\frac{\partial h}{\partial y}\right)\right) + \ldots$$

$$\ldots + \frac{\partial}{\partial z}\left(\frac{\rho k_z}{\mu}\left(\frac{\partial p}{\partial z} - \gamma\frac{\partial h}{\partial z}\right)\right) + \tilde{q}. \tag{16}$$

where $\gamma = \rho g$ is the fluid density in terms of pressure per distance (usually called fluid gravity).

2.3 Finite-Difference Approximation

The Equation (16) has only analytical solution for a simplified reservoir system. The most common numerical methods used in oil industry are based on the finite-difference method (Fitts, 2002). For this method, the reservoir is discretized in cell blocks and each cell has its own values of pressure, temperature, fluid properties and rock properties. The grid point (x_i, y_j, z_k) and spatial steps $\Delta x_i, \Delta y_j$, and Δz_k, will be simply written as (i, j, k) and $\Delta x, \Delta y$, and Δz, respectively.

2.4 Time Discretization

There are different methods for the discretization of differential equations dependent of the time, namely: explicit and implicit methods. The BTCS implicit method (backward-time, central-space) to approximate the partial derivative of the first order in time for a backward finite-difference is unconditionally stable (Chen, 2007). For this reason, we will use this approach discretize the time coordinate. Therefore, the left slide of Eq. (16) gives

$$Vc(p)\frac{\partial p}{\partial t} \approx Vc(p^{n+1})\frac{p^{n+1} - p^n}{\Delta t}, \tag{17}$$

where V is the volume of the gridblock. where the index n represents the iteration at time t_n, Δt the step time and $c(p)$ assumes different values, depending of the compressibility fluid assumption (compressible, slightly compressible or incompressible). In this case, $c(p) = \rho\phi c_t$.

2.5 Spatial Discretization

Using the central-difference approximations for the first order derivatives, and the discretization scheme shown in Fig. 2, the spatial discretization may be written as:
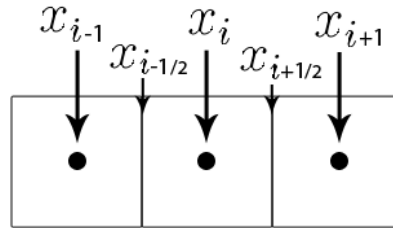

Figure 2: Spatial discretization scheme

$$\left(\frac{A_x\rho k_x}{\mu\Delta x}\right)_{i+1/2,j,k}(p_{i+1,j,k} - p_{i,j,k}) - \left(\frac{A_x\rho k_x}{\mu\Delta x}\right)_{i-1/2,j,k}(p_{i,j,k} - p_{i-1,j,k}) + \ldots$$

$$\ldots + \left(\frac{A_y\rho k_y}{\mu\Delta y}\right)_{i,j+1/2,k}(p_{i,j+1,k} - p_{i,j,k}) - \left(\frac{A_y\rho k_y}{\mu\Delta y}\right)_{i,j-1/2,k}(p_{i,j,k} - p_{i,j-1,k}) + \ldots$$

$$\ldots + \left(\frac{A_z\rho k_z}{\mu\Delta z}\right)_{i,j,k+1/2}(p_{i,j,k+1} - p_{i,j,k}) - \left(\frac{A_z\rho k_z}{\mu\Delta z}\right)_{i,j,k-1/2}(p_{i,j,k} - p_{i,j,k-1}) + \ldots$$

$$\ldots - \left(\frac{A_x\rho k_x\gamma}{\mu\Delta x}\right)_{i+1/2,j,k}(h_{i+1,j,k} - h_{i,j,k}) + \left(\frac{A_x\rho k_x\gamma}{\mu\Delta x}\right)_{i-1/2,j,k}(h_{i,j,k} - h_{i-1,j,k}) + \ldots$$

$$\ldots - \left(\frac{A_y\rho k_y\gamma}{\mu\Delta y}\right)_{i,j+1/2,k}(h_{i,j+1,k} - h_{i,j,k}) + \left(\frac{A_y\rho k_y\gamma}{\mu\Delta y}\right)_{i,j-1/2,k}(h_{i,j,k} - h_{i,j-1,k}) + \ldots$$

$$\ldots - \left(\frac{A_z\rho k_z\gamma}{\mu\Delta z}\right)_{i,j,k+1/2}(h_{i,j,k+1} - h_{i,j,k}) + \left(\frac{A_z\rho k_z\gamma}{\mu\Delta z}\right)_{i,j,k-1/2}(h_{i,j,k} - h_{i,j,k-1}) + Q_{i,j,k}, \tag{18}$$

where A_x, A_y and A_z are the cross-sectional area normal to the respective directions and $Q_{i,j,k} = \tilde{q}_{i,j,k} V_{i,j,k}$ is the injection/production.

Thus, defining *Transmissibility*:

$$T_{i+1/2,j,k} = \left(\frac{A_x \rho k_x}{\mu \Delta x} \right)_{i+1/2,j,k} . \tag{19}$$

This property depends on porous media and due to the fact that block-centered grids, the transmissibility coefficient must be evaluated on the block's boundaries. It means that permeability will be given by the harmonic average between two cells connected in series, that is:

$$(k_x)_{i\pm1/2,j,k} = \frac{2}{\frac{1}{(k_x)_{i\pm1,j,k}} + \frac{1}{(k_x)_{i,j,k}}} . \tag{20}$$

Similarly for the permeabilities in y and z. Rewriting Eq. (18) in terms of trasmissibilities:

$$T_{i+1/2,j,k}(p_{i+1,j,k} - p_{i,j,k}) - T_{i-1/2,j,k}(p_{i,j,k} - p_{i-1,j,k}) + \ldots$$

$$\ldots + T_{i,j+1/2,k}(p_{i,j+1,k} - p_{i,j,k}) - T_{i,j-1/2,k}(p_{i,j,k} - p_{i,j-1,k}) + \ldots$$

$$\ldots + T_{i,j,k+1/2}(p_{i,j,k+1} - p_{i,j,k}) - T_{i,j,k-1/2}(p_{i,j,k} - p_{i,j,k-1}) + \ldots$$

$$\ldots - \gamma T_{i+1/2,j,k}(h_{i+1,j,k} - h_{i,j,k}) + \gamma T_{i-1/2,j,k}(h_{i,j,k} - h_{i-1,j,k}) + \ldots$$

$$\ldots - \gamma T_{i,j+1/2,k}(h_{i,j+1,k} - h_{i,j,k}) + \gamma T_{i,j-1/2,k}(h_{i,j,k} - h_{i,j-1,k}) + \ldots$$

$$\ldots - \gamma T_{i,j,k+1/2}(h_{i,j,k+1} - h_{i,j,k}) + \gamma T_{i,j,k-1/2}(h_{i,j,k} - h_{i,j,k-1}) + Q_{i,j,k} . \tag{21}$$

Thus, the equation applied to each cell is given by:

$$T_{i+1/2,j,k}(p_{i+1,j,k} - p_{i,j,k}) - T_{i-1/2,j,k}(p_{i,j,k} - p_{i-1,j,k}) + \ldots$$

$$\ldots + T_{i,j+1/2,k}(p_{i,j+1,k} - p_{i,j,k}) - T_{i,j-1/2,k}(p_{i,j,k} - p_{i,j-1,k}) + \ldots$$

$$\ldots + T_{i,j,k+1/2}(p_{i,j,k+1} - p_{i,j,k}) - T_{i,j,k-1/2}(p_{i,j,k} - p_{i,j,k-1}) + \ldots$$

$$\ldots - \gamma T_{i+1/2,j,k}(h_{i+1,j,k} - h_{i,j,k}) + \gamma T_{i-1/2,j,k}(h_{i,j,k} - h_{i-1,j,k}) + \ldots$$

$$\ldots - \gamma T_{i,j+1/2,k}(h_{i,j+1,k} - h_{i,j,k}) + \gamma T_{i,j-1/2,k}(h_{i,j,k} - h_{i,j-1,k}) + \ldots$$

$$\ldots - \gamma T_{i,j,k+1/2}(h_{i,j,k+1} - h_{i,j,k}) + \gamma T_{i,j,k-1/2}(h_{i,j,k} - h_{i,j,k-1}) + Q_{i,j,k} =$$

$$V c(p^{n+1}) \frac{p^{n+1} - p^n}{\Delta t} . \tag{22}$$

CILAMCE 2016

Proceedings of the XXXVII Iberian Latin-American Congress on Computational Methods in Engineering
Suzana Moreira Ávila (Editor), ABMEC, Braslia, DF, Brazil, November 6-9, 2016

3   NUMERICAL METHOD

The numerical method proposed is based on the flow rate conservation. Every single cell which belongs to the fine grid will be considered homogeneous and isotropic.

A set of m cells at the fine grid is chosen as the cells to be upscaled for the coarse grid. The pressure field is then solved for the fine grid, and then flow rates are calculated.

The Figures 3 and 4 may help with the explanation. As can be noticed, the number of cells in a set varies. The cells that will be homogenized are hatched, this cells will be called *Upscaling Zone*. There are cell layers around the upscaling zone. This cell layers will be called *rings* and the number of rings may vary.
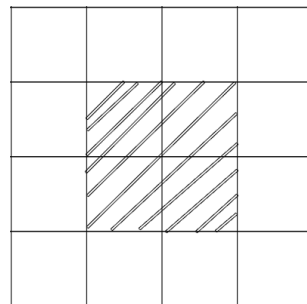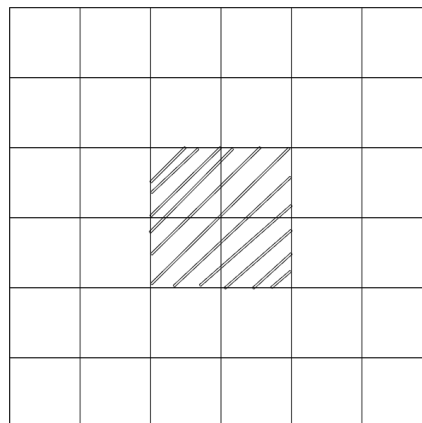
Figure 3: 4X4 set of cells

Figure 4: 6X6 set of cells

A 4x4 set of cells will be considered for this formulation, but for a higher number of rings formulation is similar. Two different sets of boundary conditions will be chosen. For the first set of boundary conditions, no-flow condition is applied at the boundaries located on the north and south of the fine grid region, and prescribed different pressures are applied on the left and right boundaries of the fine grid, the scheme is shown in Fig. 5.

A linear system comes up when finite-difference equations shown in the previous section are applied to each cell. The system has 32 unknown pressures and 32 equations. Once this system is numerically solved, the total flow in the x direction, named q_x, is known. The flow q_x is calculated in the *Principal Area* of direction x, that is the total area normal to x direction right in the middle of upscaling zone, as indicated in Fig. 5.
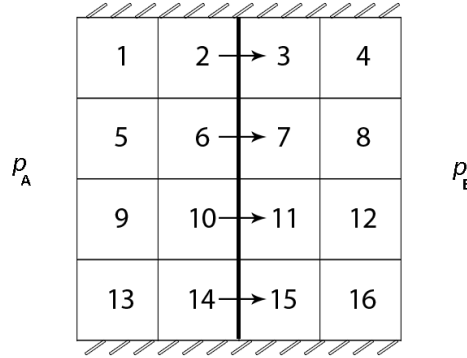
Figure 5: First set of boundary conditions, *principal area-x* indicated with a bold line, q_x indicated with arrows(p_a and p_b are prescribed pressures)

Analogously, for the second set of boundary conditions, shown in Fig. 6, the no-flow condition is applied at the east and west boundaries and the prescribed pressures are now applied on the north and south, giving rise to the flow in the y-direction, q_y. Using the same logic, q_y is calculated in the *principal area-y*.
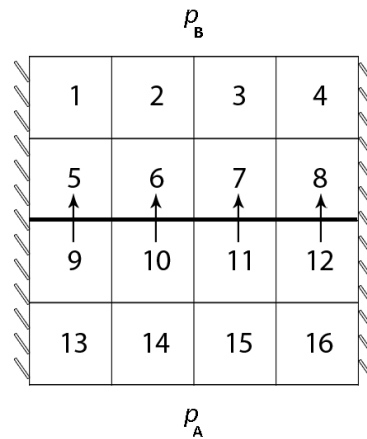

Figure 6: Second set of boundary conditions, *principal area-y* indicated with a bold line, q_y indicated with arrows(p_a and p_b are prescribed pressures)

The flows q_x and q_y are calculated in Eqs. 23 and 24:

$$q_x = \frac{\Delta z \Delta y}{\mu}\Big[(p_2^{(1)} - p_3^{(1)})k_{2,3} + (p_6^{(1)} - p_7^{(1)})k_{6,7} + (p_{10}^{(1)} - p_{11}^{(1)})k_{10,11} + $$

$$+(p_{14}^{(1)} - p_{15}^{(1)})k_{14,15}\Big], \tag{23}$$

$$q_y = \frac{\Delta z \Delta x}{\mu}\Big[(p_5^{(2)} - p_9^{(2)})k_{5,9} + (p_6^{(2)} - p_{10}^{(2)})k_{6,10} + (p_7^{(2)} - p_{11}^{(2)})k_{7,11} + $$

$$+(p_8^{(2)} - p_{12}^{(2)})k_{8,12}\Big]. \tag{24}$$

where p_i is the pressure of cell i, the index (1) e (2) are the first and second set of boundary conditions and $k_{a,b}$ is the harmonic average permeability of k_a and k_b.

With q_x and q_y calculated, it is possible to proceed. The hatched cells are going to be homogenized and now they have unknown permeabilites k_{eqx} and k_{eqy} that must be calculated. The same sets of boundary conditions are applied and a new system is formed using the finite-difference equations, the system has 32 unknown pressures, 2 unknown permeabilities and only 32 equations. It is needed two more equations to solve this system. Thus, the values of q_x and q_y are used to create the Eqs. 25 e 26.

$$q_x = \frac{\Delta z \Delta y}{\mu}\left[(p_2^{(1*)} - p_3^{(1*)})k_{2,3} + (p_6^{(1*)} - p_7^{(1*)})k_{eqx} + (p_{10}^{(1*)} - p_{11}^{(1*)})k_{eqx} + \right.$$

$$\left. +(p_{14}^{(1*)} - p_{15}^{(1*)})k_{14,15}\right], \tag{25}$$

$$q_y = \frac{\Delta z \Delta x}{\mu}\left[(p_5^{(2*)} - p_9^{(2*)})k_{5,9} + (p_6^{(2*)} - p_{10}^{(2*)})k_{eqy} + (p_7^{(2*)} - p_{11}^{(2*)})k_{eqy} + \right.$$

$$\left. +(p_8^{(2*)} - p_{12}^{(2*)})k_{8,12}\right]. \tag{26}$$

where $(1*)$ e $(2*)$ are the first and second set of boundary conditions. Furthermore, the new system is a non-linear system, and we have implemented an iterative process in order to solve this non-linear set of equations. The solution of this set of equations will result in the homogenized grid pictured in Fig.7
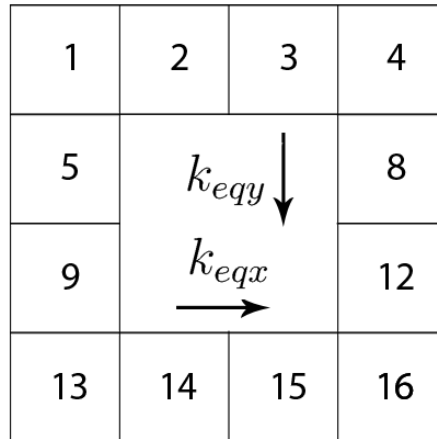

Figure 7: *Upscaling Zone* Homogenized

Usually, the set of cells after homogenization does not have the same values of pressure, but the previous pressures are a great first trial for it. And the initial trial for the new permeabilities comes from an approximation of the Eqs. 23 and 24:

$$k_{eqx,trial} \approx \frac{q_x \frac{\mu}{\Delta z \Delta y} - \left[(p_2^{(1)} - p_3^{(1)})k_{2,3} + (p_{14}^{(1)} - p_{15}^{(1)})k_{14,15}\right]}{(p_6^{(1)} - p_7^{(1)}) + (p_{10}^{(1)} - p_{11}^{(1)})}, \tag{27}$$

$$k_{eqy,trial} \approx \frac{q_y \frac{\mu}{\Delta z \Delta x} - \left[(p_5^{(2)} - p_9^{(2)})k_{5,9} + (p_8^{(2)} - p_{12}^{(2)})k_{8,12}\right]}{(p_6^{(2)} - p_{10}^{(2)}) + (p_7^{(2)} - p_{11}^{(2)})}. \tag{28}$$

Numerical methods based on iterative cycles may present some convergence and stability problems. However, achieving the convergence can depend on the first trial values that have to be chosen or calculated.

The final result will exhibit equivalent permeabilities in x and y directions, and this is the main feature of this technique: less cells to evaluate with a possibly higher degree of anisotropy.

4 NUMERICAL RESULTS

The numerical upscaling method previously presented is evaluated in some 2D permeability fields. In order to assess performance of number of rings, the simulations are made using 1 ring and 2 rings, and its results are compared to simulations made on meshs generated by harmonic and arithmetic average, which is a classical method used in petroleum industry because of its simplicity. The parameter used for evaluating methods is the produced volume in 5 days. The first permeability field used is a random generated mesh. After, the upscaling method is applied to a log-normal permeability field. Moreover, the performance of the upscaling method is analyzed for a SPE's dataset, available on the SPE's website.

The error analyses in all cases is calculated as

$$E_p = \left| \frac{V_{coarse} - V_{fine}}{V_{fine}} \right| \times 100. \tag{29}$$

4.1 Random distribution

The first model studied is a square two-dimension matrix (20x20) randomly generated. In figure 8, a scheme shows the production wells placed in two locations, location 1 and 2. It is important to say that the wells are not producing at the same time. Each well is a different simulation. The paramenters of the simulation are shown in Table 1 and the volume, error and time reducing results are shown in Table 2.
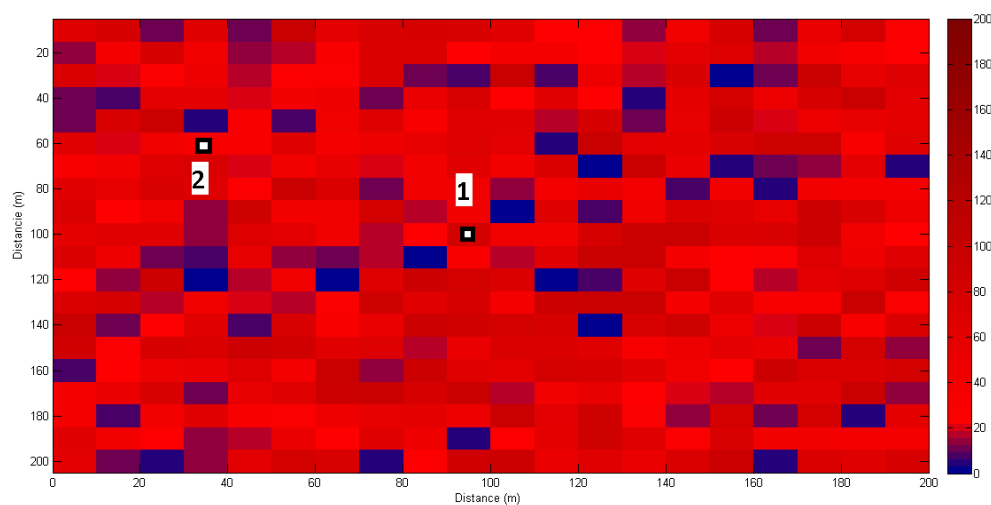

Figure 8: 20X20 Random permeability field, wells indicated by squares

Table 1: Simulation parameters of random distribution mesh

Number of Upscalings	0	1	2
Simulation time (s)	2.54	0.11	0.01
Number of Cells	400	100	25
Cell Volume ($m \times m \times m$)	10 X 10 X 1	20 X 20 X 1	40 X 40 X 1
Homogenization Time (Average)	-	0.00	0.00
Homogenization Time (s) (1 ring)	-	18.94	2.61
Homogenization Time (s) (2 rings)	-	19.93	4.35

Simulation time, presented in table 1 is the average time of simulation in this mesh, in other words, time spent on solving the system of discretized equations. Homogenization time is the time spent on the generation of coarse grid based on the original grid, this step occur before the simulation.

Table 2: Simulation results of a random distribution mesh in terms of volume

	1 Upscaling		2 Upscalings	
Well Location	1	2	1	2
Volume (m^3) (Original)	1.780	1.744	1.780	1.744
Volume (m^3) (average)	1.706	1.701	1.690	1.701
Error (average)	4.27	2.46	5.27	2.46
Volume (m^3) (1 ring)	1.709	1.696	1.688	1.700
Error (1 ring)	4.13	2.73	5.38	2.56
Volume (m^3) (2 rings)	1.709	1.696	1.693	1.698
Error (2 rings)	4.10	2.73	5.10	2.64

The results do not shown significant difference between average upscaling and ring upscaling. It is remarkable the great reduction of simulation time using upscaling techniques.

4.2   Log-normal distribution

The second model studied is a square two-dimension matrix (40x40) with a log-normal probability distribution of the permeability. In figure 9, a scheme shows the production wells placed in two locations, location 1 and 2. Again, the wells are not producing at the same time.

The paramenters of the simulation are shown in Table 3 and the volume, error and time reducing results are shown in Table 4.
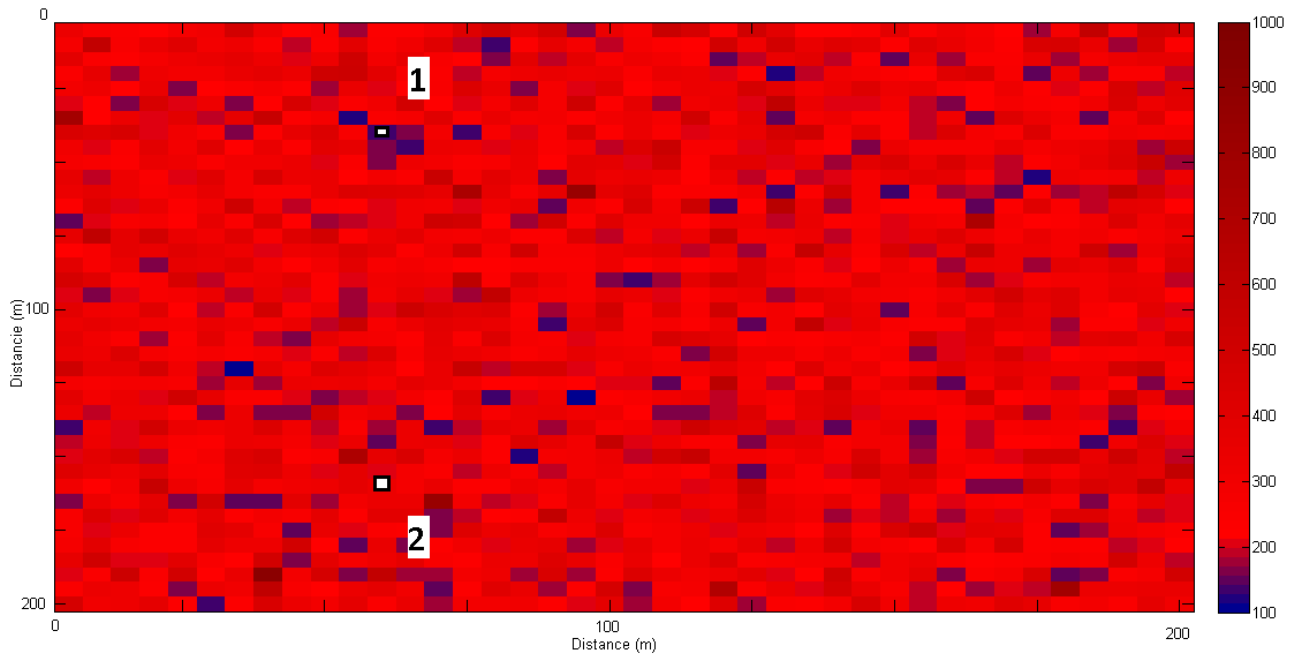

Figure 9: 40X40 Log-Normal permeability field, wells indicated by squares

Table 3: Simulation parameters of log-normal distribution mesh

Number of Upscalings	0	1	2
Simulation time (s)	116.37	2.50	0.12
Number of Cells	1600	400	100
Cell Volume ($m \times m \times m$)	10 X 10 X 1	20 X 20 X 1	40 X 40 X 1
Homogenization Time (Average)	-	0.00	0.00
Homogenization Time (s) (1 ring)	-	33.62	7.47
Homogenization Time (s) (2 rings)	-	73.29	16.22

Again, the results do not shown (Table 4) significant difference between average upscaling and ring upscaling. Moreover, the error in location 1 is greater than location 2. Analysing the Fig. 9, it happens because the location 1 has more heterogeneity than location 2.

Table 4: Simulation results of a log-normal distribution mesh in terms of volume

	1 Upscaling		2 Upscalings	
Well Location	1	2	1	2
Volume (m^3) (Original)	7.825	6.843	7.825	6.843
Volume (m^3) (Average)	7.889	6.871	6.951	6.940
Error (Average)	9.33	0.41	11.16	1.41
Volume (m^3)(1 ring)	7.905	6.878	6.959	6.940
Error (1 ring)	9.13	0.52	11.06	1.41
Volume (m^3) (2 rings)	7.104	6.879	6.957	6.941
Error (2 rings)	9.22	0.53	11.08	1.43

4.3 SPE Datasets

This model was obtained from *SPE Comparative Solution Project (SPE, 2001)*. The datasets of this project was developed as a benchmark to compare the performance of different methods or algorithms held in Houston, Texas, in February of 2001. In particular, interest was placed in studying the behavior of upscaling and upgridding algorithms for the computation of the permeability fields.

SPE dataset 1: is a two-phase (oil and gas) and the computational domain is a vertical cross-section without dipping and faults. The dimension of the model are $\Delta x = 7,62m$; $\Delta y = 7,62m$ and $\Delta z = 0,762m$. The fine scale grid 100x1x20 with uniform size for each of the grid blocks. In the present work, the mono-phase model with incompressible and immiscible fluid has to be considered and the permeability distribution is a correlated geostastically generated field with constant porosity ϕ=0,2. The size of cells were changed to are $\Delta x = 20m$; $\Delta y = 20m$ and $\Delta z = 2m$.

In figure 10, a scheme shows the production wells placed in four different locations. The paramenters of the simulation are shown in Table 5 and the volume, error and time reducing results are shown in Table 6.

A significant improvement in the results is noticed in table 6. Specially for the 2 rings upscaling, the errors were quite small. This effect is due to the fact that this well lose few permeability and flux information because it passes thorough the entire model and upscaling does not affect it so hard.

The second, third and fourth locations are remarkable because they are more heterogeneous areas and have few information about the global flux and the results show very different values of errors. For location 3 and 4 the use of 2 rings upscaling led to a lesser error. In exception, for location 2, the classical average method had the best results.
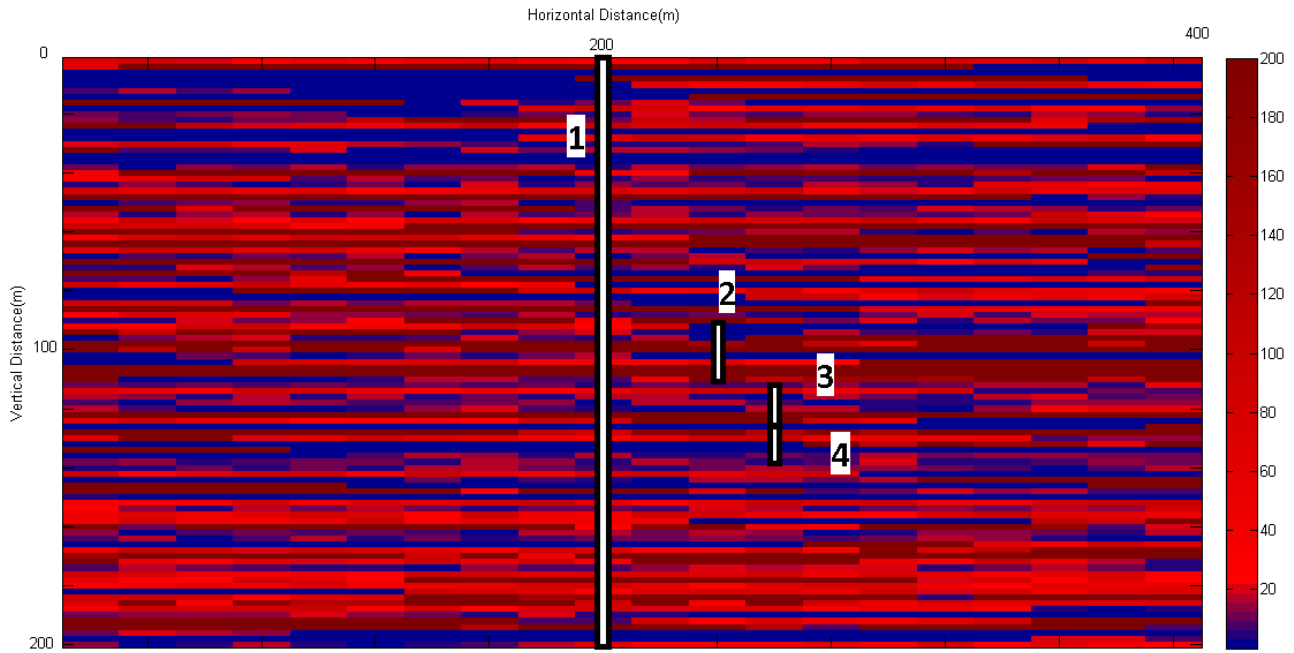
Figure 10: SPE dataset 1, wells indicated by squares

Table 5: Simulation parameters of SPE mesh

Number of Upscalings	0	1	2
Simulation time (s)	19	0.41	0.02
Number of Cells	2000	500	125
Cell Volume($m \times m \times m$)	20 X 20 X 2	40 X 40 X 2	80 X 80 X 2
Homogenization Time (Average)	-	0.00129	0.00035
Homogenization Time (s) (1 ring)	-	210.00	37.60
Homogenization Time (s) (2 rings)	-	1274.70	71.13

An important rationality comes up from the 1 and 2 rings results. When homogenization is being made, two kinds of steady state boundary conditions are set, but, into the real mesh this set of cells is exposed to another boundary conditions, and these boundary conditions may vary depending on reservoir flow state. So, the higher the number of rings around the *upscaling zone* the lesser is the boundary condition influence, therefore, the error is smaller.

The homogenization time of SPE dataset 1 had the worst results and it gets even worse when the number of rings is higher. The main reason is that the non-linear system gets ill-conditioned and sensitive to the first trial. When the system does not converge, the algorithm gives a new trial and the most of the computational cost is due to several trials to reach convergence.

Table 6: Simulation results of a SPE mesh in terms of volume

	1 Upscaling				2 Upscalings			
Well Location	1	2	3	4	1	2	3	4
Volume (Original)(m^3)	283.6	191.3	187.1	95.88	283.6	191.3	187.1	95.88
Volume (m^3)(Average)	268.3	188.0	182.7	81.59	258.0	187.4	172.1	81.72
Error (Average)	5.39	1.72	2.37	14.91	9.01	2.05	8.05	14.77
Volume (m^3)(1 ring)	284.6	182.2	166.1	87.30	275.0	188.8	168.0	81.34
Error (1 ring)	0.33	4.75	11.23	8.95	3.05	1.32	10.24	15.17
Volume (m^3)(2 rings)	278.7	175.1	187.0	88.27	269.6	195.1	182.5	98.97
Error (2 rings)	1.72	8.48	0.08	7.94	4.93	1.95	2.47	3.22

5 CONCLUSIONS

A technique for upscaling of absolute permeability based on conservation of flow rate was developed and extended. The results was compared to an simpler method in order to evaluate it.

In upscaling, there is not a method that works in all cases. It depends on situation. The results obtained showed us that is true. For certain cases, the simplest method was better, in others, the most sophisticated. The number of rings around the upscaling zone proved to be signifficant, especially in SPE dataset 1 case, a greater number of rings, in some locations, resulted in a noticeable improvement of results. As the results showed, increasing number of rings makes the influence of boundary conditions lesser and it leads to a better result.

As expected, the more heterogeneous is the medium the worst results are. However, for some particular cases, even if the region is quite heterogeneous the error is small. The heterogeneity also leads to a higher instability in the system and it costs a higher time to compute permeability value.

It is left as suggestions for future works: i) developing more efficient algorithms for this method, in certain cases, the method had better results, but the homogenization time was far higher than a simpler method. ii) this numerical technique can also be improved and extended to more general cases such as multi-phase flows.

REFERENCES

Chen, Z., 2007. Reservoir Simulation: Mathematical Techniques in Oil Recovery, *Society for Industrial and Applied Mathematics*, Conference Series in Applied Mathematics.

Failla, A., 2015. *A Numerical Upscaling Technique for Absolute Permeability and Single-Phase Flow Based on the Finite-Difference Method*, PhD Thesis, Politecnico di Milano

CILAMCE 2016

Proceedings of the *XXXVII Iberian Latin-American Congress on Computational Methods in Engineering*
Suzana Moreira Ávila (Editor), ABMEC, Braslia, DF, Brazil, November 6-9, 2016

Christie, M. A., 1996. Upscaling for Reservoir Simulation. *SPE, BP Exploration.*

Fitts, C. R., 2002. *Laminar and Turbulent Flow*, Groundwater Science, London, Academic press., Elsevier Science LTD, pp. 46-49.

Odster, L. V., 2013. *Numerical Aspects of Flow Based Local Upscaling.* Norwegian University of Science and Technology, Trondheim.

Renard, P., Marsily, G., 2000. *Calculating equivalent permeability: A Review*, Water Resour. Res., vol. 20, pp. 261-262.

Society of Petroleum Engineers- *SPE Comparative Solution Project.* http://www.spe.org/csp, 2001, also https://www.onepetro.org/journal-paper/SPE-72469-PA.

Wen, X.H., Gmez-Hernndez, J.J., 1996. *Upscaling hydraulic conductivities in heterogeneous media: An overview*, Journal Hydrology, vol. 183, n 1-2, pp.ix-xxxii.

White, C. D., Horne, R. N., 1987. *Compting Absolute Transmissibility in the Presence of Fine-Scale Heterogeneity*, Society of Petroleum Engineering Journal, Ninth SPE Symposium on Reservoir Simulation, Society of Petroleum Engineers, pp. 209-220.